Immunometabolic Reprogramming of Monocytes in Tuberculosis Infection and Disease

Gráinne Jameson[1], Isabella Batten[1], Adam H. Dyer[1], Caoimhe Geoghegan[3], Moninne Murray[3], Niamh McDonnell[3], Dearbhla M. Murphy[1], Sarah A. Connolly[1], Anne Marie McLaughlin[2,3], Cilian Ó. Maoldomhnaigh[1], Laura E. Gleeson[1,3], Joseph Keane[1,2,3], Sharee A. Basdeo[1]

[1]School of Medicine, Trinity Translational Medicine Institute, St James' Hospital, Trinity College Dublin, Dublin, Ireland.
[2]National Tuberculosis Centre, Department of Respiratory Medicine, St James's Hospital, Dublin, Ireland.
[3]Respiratory Department, St James's Hospital, Dublin 8, Dublin, Ireland.

Corresponding author:
Gráinne Jameson
Trinity Translational Medicine Institute,
Trinity Centre for Health Sciences,
St. James's Hospital,
Dublin 8
GJAMESON@TCD.IE, +353 1 896 3263

Authors Contributions:
G.J. and S.A.B. conceived the study and hypotheses. G.J., I.B., A.H.D., C.G., M.M., N.M., A.M., L.E.G. and J.K. participated in data collection. J.K, L.E.G., C.O.M. and A.M. provided domain expert advice and evaluation of the project. G.J., I.B., A.H.D., D.M., S.A.C., C.O.M. and S.A.B. performed data and statistical analyses. All authors interpreted the data. G.J. and S.A.B. wrote the initial draft of the manuscript. All authors provided substantive critical reviews and approved of the submitted manuscript.

Sources of Support: This work was funded by the Health Research Board Ireland (HRB-ILP-POR-2022-033 and HRB-EIA-2019-010) and The Royal City of Dublin Hospital Trust (RCDH app 185). The following reagent was obtained through BEI Resources, NIAID, NIH: Mycobacterium tuberculosis, Strain H37Rv, Gamma-Irradiated Whole Cells, NR-49098).

Abstract:

Rationale:

Tuberculosis remains the leading cause of death from an infectious disease, caused by *Mycobacterium tuberculosis*. The term “latent tuberculosis infection” has been redefined as “tuberculosis infection,” reflecting immune recognition without clinical disease. Monocytes play a critical role in the innate immune response to *Mycobacterium tuberculosis*, both in the blood and in the lung, where they can repopulate the alveolar macrophage niche. However, it is unknown whether tuberculosis infection is associated with a distinct immunometabolic monocyte profile and how treatment impacts monocyte function.

Objectives:

To define blood monocyte phenotype and metabolism in individuals with tuberculosis infection and tuberculosis disease, and to evaluate the impact of treatment on monocyte metabolic function.

Measurements:

Circulating monocytes from individuals with tuberculosis infection, tuberculosis disease, and healthy controls were analysed ex vivo and following *Mycobacterium tuberculosis* stimulation. We assessed surface phenotype, cytokine and chemokine production, and metabolic activity. Groups were stratified based on treatment status.

Main Results:

Monocytes from individuals with tuberculosis infection and tuberculosis disease were functionally similar to each other but distinct from healthy controls. Both groups exhibited reduced mitochondrial dependence, which was restored in people receiving treatment. Upon stimulation with *Mycobacterium tuberculosis*, only monocytes from individuals with tuberculosis infection demonstrated enhanced metabolic activity and reduced mitochondrial dependence, along with a unique functional profile.

Conclusions:

Tuberculosis infection induces a distinct immunometabolic monocyte signature that may be reversible with treatment. These findings support the clinical relevance of tuberculosis infection and the potential for targeting monocytes through host-directed therapies.

Key words: Mycobacterium tuberculosis, Mitochondria, Innate Immunity

Introduction

Tuberculosis (TB) is the leading cause of death by an infectious agent, with an estimated 1.25 million deaths and 10.8 million cases in 2023 (1). In an effort to better reflect the spectrum of disease and infection, the World Health Organization (WHO) recently updated its terminology in the *Consolidated Guidelines on Tuberculosis* (2) in line with the International Consensus for Early TB (ICE-TB) consortium's new framework (3). Individuals with a persistent immune response to *Mycobacterium tuberculosis* (Mtb) antigens, but without clinical or radiographic evidence of active TB, are now classified as having *TB infection* (TBI), replacing the historical term "latent TB infection" (LTBI). While most individuals with TBI are asymptomatic, they remain at risk of progressing to *TB disease* (TBD)—the new term for what was previously called "active TB."

Monocytes are short-lived circulating myeloid cells that play a critical role in the peripheral immune response to infection. They possess antimicrobial functions such as phagocytosis, cytokine production, and antigen presentation (4–8). In TB, monocytes are recruited from circulation to the lungs—the primary site of infection—where they differentiate into alveolar macrophages (AMs) (9–13). The AM niche almost exclusively harbours early Mtb infection and acts as the first line of defence (14,15). Despite their crucial role in both systemic and local immune responses, how monocyte function and metabolism are altered across the TB spectrum remains poorly understood.

66 In this study, we investigated whether TBI and TBD differentially affect circulating
67 monocytes. We found that monocytes from individuals with TBI and TBD were
68 phenotypically and functionally similar ex vivo, yet distinct from healthy controls (HC).
69 Importantly, both TBI and TBD were associated with reduced mitochondrial dependence
70 (MD) in monocytes—an effect that was reversed in individuals receiving TB preventive
71 treatment (TPT) and in those after the intensive phase of TB therapy.
72
73 In response to Mtb, only monocytes from people with TBI exhibited enhanced metabolic
74 activity, supporting a potential memory-like response. These monocytes also exhibited
75 metabolic plasticity, efficiently reducing their MD in response to Mtb. Conversely,
76 monocytes from people with TBD fail to reduce their MD in response to Mtb, suggesting
77 potential mitochondrial dysfunction. Our findings indicate that infection with TB induces an
78 immunometabolic signature in monocytes from people with both TBI and TBD, which is
79 reversed with treatment. Furthermore, monocytes from TBI individuals exhibit memory-
80 like metabolic properties in their response to Mtb.
81
82

83 Methods

84

85 *Sex as a biological variable*

86 Our study examined male and female humans, and similar findings were observed for
87 both sexes.

88

89 *Human Participants*

90 All peripheral blood patient samples were collected in the out-patient department of St
91 James Hospital Dublin when patients were attending routine appointments (Table 1).
92 Written informed consent was obtained prior to collection. Exclusion criteria included age
93 under 18 years, inability to provide written informed consent, multi-drug-resistant
94 tuberculosis, or a known (or ensuing) diagnosis of malignancy, HIV or any other infection.
95 Patients undergoing biopsy as part of bronchoscopy were also excluded. Individuals with
96 TBI were divided into those pre-treatment (TBI/-; n=6) and those on-treatment (TBI/+;
97 n=4), while those with TBD were grouped into intensive (TBD/I, <2 months treatment of
98 3-4 drugs; n=4) and continuous (TBD/C, >2 months reduced to 1-2 drugs; n=4) treatment
99 phases. Peripheral blood samples were also obtained from healthy controls.

100

101 *PBMC and Monocyte Isolations*

102 PBMC were isolated from peripheral blood samples by density centrifugation over
103 Lymphoprep (StemCell Technologies). Monocytes were separated by hyperosmotic
104 density gradient centrifugation by layering PBMCs on top of a fresh hyperosmotic Percoll
105 solution (48.5% Percoll, 41.5% sterile H2O, 0.16 M NaCl) and centrifuged for 15 minutes
106 at 580*g*. The interphase layer was isolated, and cells were washed with cold PBS and
107 resuspended at a concentration of 1×10^6 cells/mL. Cells were plastic adhered for 1hr in
108 serum-free media and washed twice with PBS to remove any non-adherent cells.

109

110 Irradiated H37Rv (iH37Rv; gifted by BEI Resources) stocks were thawed, sonicated for
111 15 mins and syringed three times through a 25G needle break up clumps. iH37Rv was
112 centrifuged at 30 xg for 5 mins to pellet any further clumps. Supernatant was aspirated
113 and the concentration of iH37Rv was calculated using Pierce™ BCA Protein Assay with
114 Albumin protein as a control (Thermo Scientific™). Cells were stimulated with 10ug/mL of
115 iH37Rv overnight for 18-24hrs. Cells were left unstimulated as a control.
116

117 *Cytokine and Chemokine Analyses*

118 A Human Luminex Discovery Kit (Cat LXSAHM-25) was designed to assess the following
119 analytes in monocyte supernatants: CCL1/I-309/TCA-3 (BR15), CCL2/JE/MCP-1 (BR25),
120 CCL3/MIP-1 alpha (BR35), CCL4/MIP-1 beta (BR37), CXCL1/GRO alpha/KC/CINC-1
121 (BR77), CXCL2/GRO beta/MIP-2/CINC-3 (BR27), CXCL9/MIG (BR52), CXCL10/IP-
122 10/CRG-2 (BR67), G-CSF (BR54), GM-CSF (BR46), Granzyme B (BR57), IFN-alpha
123 (BR63), IFN-beta (BR21), IFN-gamma (BR29), IL-1 alpha/IL-1F1 (BR38), IL-1 beta/IL-1F2
124 (BR28), IL-1ra/IL-1F3 (BR30), IL-6 (BR13), IL-8/CXCL8 (BR18), IL-10 (BR22), IL-12 p70
125 (BR56), IL-17/IL-17A (BR42), IL-18/IL-1F4 (BR78), IL-23 (BR76), TNF-alpha (BR12).
126 Assay was carried out as per manufacturers protocol and analysed on Luminex MAGPIX
127 System. Unstimulated and Mtb-stimulated cells from each donor were analyzed
128 concurrently on the same plate, thereby eliminating potential inter-assay variability and
129 ensuring the accurate calculation of fold-change values. Analyte concentrations were
130 determined based on standards supplied in the kit, with a 5 parameter logistic regression
131 (5-PL) curve used on xPONENT(TM) software.
132

133 *Flow cytometry*

134 For phenotypical analyses PBMCs were resuspended in PBS (Gibco) and stained
135 immediately. Anti-CD86 BV421 (1:100, IT2.2), anti-CD45RA BV711 (1:100, HI100), anti-
136 CD40 APCCy7 (1:100, 5C3), anti-HLADR APC (1:100, L243), anti-CD14 AlexaFlour 488
137 (1:100, HCD14), anti-CD16 PerCpCy5.5 (1:100, 3G8), anti-CD80 PeCy7 (1:100, 2D10),
138 anti-TNFRI PE (1:50, W15099A), and anti-TNFRII PeDazzle594 (1:100, 3G7A02) were
139 purchased from Biolegend and added to the cells for 10 mins at RT. Cells were washed,
140 fixed and acquired or stored at 4°C until acquisition.

141

142 Cultured PBMCs were resuspended in 100µl of FcR block (1µl/test; Miltenyi Biotec) and
143 ZombieNIR stain (Biolegend) in 1X PBS (Gibco). Cells were then surface stained with
144 anti-CD14 and permeabilized with Foxp3 staining kit (eBioscience) according to the
145 manufacturer's instructions. Cells were incubated for 30 mins at 4°C with anti-puromycin
146 (1:100, 2A4; Biolegend). Cells were acquired on a FACS Canto (BD Biosciences), BD
147 Fortessa, (BD Biosciences) or an Amnis CellStream (Luminex Corporation, Austin, TX,
148 USA). All data analysis was performed using FlowJo software (BD Biosciences).

149

150 *SCENITH (Single Cell mEtabolism by profiling Translation inHibition)*

151 This protocol utilises puromycin as a surrogate for protein synthesis as it is incorporated
152 into nascent proteins. By using specific metabolic inhibitors and measuring puromycin
153 incorporation we can estimate the glycolytic capacity (GC), mitochondrial dependence
154 (MD), fatty acid and amino acid oxidation capacity (FAO/AAOC) and glucose dependence
155 (GD) of cells at the single cell level as previously described(16). Post 18hrs of culture,

156 SCENITH metabolic function profiling was carried out on PBMCs. Cells were treated for
157 40 mins at 37°C, 5% CO2 with DMSO Control (Co, 0.02% DMSO), 2-Deoxy-D-Glucose
158 (DG; 100mM; Sigma-Aldrich), Oligomycin (O; 1μM; Sigma-Aldrich), a combination of both
159 drugs (DGO), or with a negative control (Harringtonine; Sigma-Aldrich; 2ug/ml).
160 Puromycin (Puro; 10μg/mL; Sigma-Aldrich) was added for the final 35 mins. Cells were
161 washed in PBS and flow cytometry staining was carried out. The following calculations
162 were used:
163
164 Co = GeoMFI of anti-Puro-Fluorochrome upon Control treatment.
165 DG = GeoMFI of anti-Puro-Fluorochrome upon 2-Deoxy-D-Glucose treatment.
166 O = GeoMFI of anti-Puro-Fluorochrome upon Oligomycin A treatment.
167 DGO = GeoMFI of anti-Puro-Fluorochrome upon DG+O treatment.
168
169 Mitochondrial Dependence (MD)=100(Co-O)/(Co-DGO)
170 Glycolytic Capacity (GC)= 100-100(Co-O)/(Co-DGO)
171 Fatty Acid and Amino Acid Oxidation Capacity (FAOC)= 100-(100(Co-DG)/(Co-DGO)
172 Glucose Dependence (GD)= 100(Co-DG)/(Co-DGO)
173 Therefore, GC is the inverse data of MD (i.e. GC= 100- MD) and FAOC is the inverse data
174 of GD (i.e. FAOC= 100-GD). Patient samples with sufficient cell numbers underwent
175 metabolic profiling. No data was omitted.
176

177 *Statistics*

178 Statistical analysis was performed using GraphPad Prism version 10. The statistical test
179 used is indicated in each Fig. legend. A P-value of <0.05 was considered significant.

180

181 *Study Approval*

182 Our study protocol was approved by the Joint Research Ethics Committee of St. James's
183 and Tallaght Hospitals and by Trinity College Dublin. Written informed consent was
184 received from participants prior to inclusion in the study

185

186 *Data availability*

187 Data is available directly from the corresponding author.

188

189

190 Results

191

192 **Monocytes from individuals with TBI and TBD are functionally similar but distinct**
193 **from HC, both ex vivo and following Mtb stimulation.**

194

195 To assess monocyte functional differences across the TB spectrum, monocytes were
196 isolated from peripheral blood mononuclear cells (PBMC) and cultured for 18 hours with
197 or without Mtb. Supernatants were harvested, and cytokine/chemokine levels were
198 quantified using Luminex multiplex custom bead-based immunoassay (Figure 1). The

199 cytokine and chemokine profile of unstimulated monocytes from individuals with TBI (light
200 grey) and TBD (dark grey) was distinct from that of healthy controls (HC; blue) (Figure1 A
201 and Supplemental Figure 1A).
202
203 Upon Mtb stimulation, monocytes from both TBI and TBD individuals produced
204 significantly higher concentrations of several cytokines and chemokines compared with
205 HC, with no significant differences observed between the TBI and TBD groups (Figure 1B-
206 C and Supplemental Figure 1B). Specifically, monocytes from individuals with TBI
207 demonstrated significantly greater fold increases in IL-1α (P= 0.0153), IL-8 (P= 0.0129),
208 IL-17A (P= 0.0171), IL-18 (P= 0.0438), IL-23 (P= 0.0158), IFN-γ (P= 0.0382), GM-CSF (P=
209 0.0346), ILRA (P= 0.0084), CXCL1 (P= 0.0194), CXCL9 (P= 0.0129), and CCL2 (P=
210 0.0420) compared to HC (Figure 1C). Similarly, TBD monocytes exhibited significantly
211 higher fold increases in IL-1α (P=0.0228), IL-6 (P=0.0260), IL-8 (P=0.0278), IL-23
212 (P=0.0400), GM-CSF (P=0.0203), CCL3 (P=0.0318), and CCL4 (P=0.0388) compared
213 with HC (Figure 1C). Monocytes from people with TBI and TBD exhibit similar functional
214 responses to Mtb stimulation distinct from HC.
215
216 **Monocytes from individuals with TBI and TBD are phenotypically similar but**
217 **distinct from HC ex vivo.**
218 To assess whether TBI or TBD differentially influence monocyte frequency or phenotype,
219 we analyzed PBMC from individuals with TBI, TBD, and HC by flow cytometry.
220 Granulocyte frequencies were significantly elevated in both TBI and TBD groups
221 compared with HC (TBI: P=0.0303; TBD: P=0.0120; Figure 2A). In contrast, no significant

222 differences were observed in the frequencies of classical, intermediate, or non-classical
223 monocyte subsets across groups (Figure 2B).
224
225 Phenotypic analysis revealed increased expression of CD14 and CD45RA on classical
226 monocytes from individuals with TBI (CD14: P=0.0039; CD45RA: P=0.0070) and TBD
227 (CD14: = 0.0010; CD45RA: P=0.0007) compared with HC (Figure 2D). Conversely, HLA-
228 DR expression was significantly reduced on classical monocytes from both TBI (P =
229 0.0374) and TBD (P<0.0001) individuals relative to HC. Expression of TNFRI and TNFRII
230 was also significantly decreased on classical monocytes in the TBI group (TNFRI:
231 P=0.0185; TNFRII: P = 0.0414; Figure 2D). Similar phenotypic changes were observed in
232 intermediate and non-classical monocyte subsets (Supplemental Figure 2). These
233 findings demonstrate a shared, altered monocyte phenotype in TBI and TBD individuals,
234 distinct from that of healthy controls.
235
236 **Infection with TB reduces monocyte mitochondrial dependence in people with TBI**
237 **pre-treatment and people with TBD in intensive treatment phase.**
238 We next compared the metabolic function of monocytes from HC and individuals with TBI
239 or TBD using the SCENITH protocol, which leverages puromycin incorporation as a proxy
240 for protein synthesis—representing approximately 50% of a cell's total metabolic activity
241 (Figure 3A). In unstimulated monocytes, no significant differences in protein synthesis
242 were observed between groups (Figure 3B).
243

244 To assess MD, monocytes were treated with oligomycin, and their glycolytic capacity was
245 calculated using SCENITH analysis (see Methods for details). Monocytes from HC
246 showed high MD and correspondingly low glycolytic capacity. In contrast, monocytes from
247 individuals with TBI or TBD exhibited significantly reduced MD (TBI P=0.01, TBD
248 P=0.0078; Figure 3C).
249
250 To evaluate glucose dependency, cells were treated with 2-deoxyglucose (2DG). The
251 SCENITH-derived calculation for alternative fuel use (fatty acids and amino acids) showed
252 no significant differences across groups. Monocytes from all groups demonstrated high
253 glucose dependence (Figure 3C).
254
255 We further stratified participants based on treatment status. Individuals with TBI were
256 divided into pre-treatment (TBI/-) and on-treatment (TBI/+), while those with TBD were
257 grouped into intensive (TBD/I, <2 months treatment of 3-4 drugs) and continuous (TBD/C,
258 >2 months treatment reduced to 1-2 drugs) treatment phases. No differences in protein
259 synthesis were observed between these stratified groups (Figure 3D). However,
260 monocytes from TBI/- individuals exhibited significantly lower MD compared with HC,
261 whereas TBI/+ monocytes did not differ significantly from HC (P=0.0258; Figure 3E).
262 Similarly, TBD/I monocytes had significantly reduced MD compared to HC (P=0.0198),
263 while TBD/C monocytes did not (Figure 3E). These findings suggest that both TPT and
264 TBD treatment may help restore monocyte metabolic function toward that of HC.
265

266 **Monocytes from people with TBI and TBD exhibit divergent metabolic responses to**
267 **Mtb.**
268 Given the distinct clinical and immunological outcomes between TBI and TBD, we
269 hypothesized that their monocyte metabolic responses to Mtb would differ. Despite
270 reduced MD in unstimulated monocytes from both TBI and TBD individuals, their
271 metabolic responses to Mtb stimulation were similar to HC, characterized overall by low
272 MD and high glucose dependence (Figure 3F).
273
274 Interestingly, only monocytes from TBI individuals showed a significant increase in
275 puromycin MFI in response to Mtb, indicating elevated protein synthesis and metabolic
276 activity (P=0.0008; Figure 3G). This effect remained significant when stratified by TPT
277 status in both TBI/- (P = 0.0137) and TBI/+ (P = 0.0024) subgroups (Figure 3H).
278
279 In response to Mtb, MD was significantly reduced in HC (P=0.0021) and TBI (P=0.0023)
280 monocytes, but not in those from TBD individuals (Figure 3I). Within the TBI group,
281 monocytes from TBI/- individuals had lower baseline MD than those from TBI/+ individuals
282 (P = 0.0108). Nevertheless, monocytes from both subgroups showed a significant
283 reduction in MD following Mtb stimulation (TBI/- P = 0.0217; TBI/+ P = 0.0057; Figure 3J).
284
285 Similarly, in the TBD group, monocytes from individuals in the intensive treatment phase
286 (TBD/I) displayed lower baseline MD compared to those in the continuous treatment
287 phase (TBD/C; P = 0.0447; Figure 3K). However, Mtb stimulation did not induce a
288 significant change in MD in either TBD subgroup (Figure 3K). Collectively, these findings

289 reveal key differences in the metabolic response of monocytes to Mtb between TBI and
290 TBD individuals and suggest that monocytes from those with TBI may exhibit memory-like
291 responses to Mtb.
292
293

294 Discussion

295 In this study, we provide new insight into how TB infection, whether clinically symptomatic
296 or not, impacts human monocyte phenotype, function and metabolism. By comparing
297 peripheral blood monocytes from individuals with TBI, TBD, and uninfected HC, we
298 demonstrate that TB infection induces sustained alterations in monocyte profiles, even in
299 the absence of clinical disease. Monocytes from individuals with TBI exhibit changes in
300 cytokine and chemokine production, surface marker expression, and a reduced MD—
301 closely resembling patterns observed in TBD. Importantly, we demonstrate that treatment,
302 including TPT, can partially restore monocyte metabolism toward a profile more similar to
303 that of healthy individuals. These shared features indicate that myeloid immunometabolic
304 reprogramming occurs early in TB infection and persists without clinical disease.
305
306 Specifically, we observed divergent metabolic responses between TBI and TBD
307 monocytes, both at baseline and upon in vitro Mtb stimulation. At baseline, monocytes
308 from people with both TBI and TBD exhibited significantly lower MD compared with HC,
309 potentially indicating a metabolic shift toward glycolysis- a hallmark of heightened
310 activation (17). However, overall metabolic activity remained comparable across all
311 groups at baseline, suggesting similar activation levels. Cytokine and chemokine profiling

312 of unstimulated monocytes supports this interpretation, with TBI and TBD monocytes
313 producing elevated levels of IL-17A and CXCL9, but reduced levels of IL-1β and CXCL2
314 relative to HC. This reduced MD may also reflect underlying mitochondrial dysfunction,
315 particularly in TBD, where chronic immune activation could drive energetic exhaustion.
316 Notably, monocytes from people with TBI and TBD who are receiving treatment do not
317 exhibit reduced MD, suggesting that current therapeutic strategies may help re-establish
318 myeloid immunometabolic homeostasis. These findings also highlight the potential of
319 using monocyte MD as a clinical indicator of treatment response in individuals with TBI.
320
321 Upon Mtb stimulation, monocytes from individuals with TBI mounted the expected
322 metabolic shift, characterised by increased protein synthesis and reduced MD, consistent
323 with a glycolytic response. In contrast, monocytes from individuals with TBD failed to
324 exhibit this metabolic shift, indicating impaired metabolic plasticity. This inability to engage
325 glycolysis in the context of active infection may reflect an exhausted or dysregulated
326 metabolic state, potentially contributing to ineffective pathogen control or persistent
327 inflammation. These findings suggest that metabolic plasticity is a feature of controlled
328 infection (TBI), whereas rigid or dysfunctional metabolism may characterize disease
329 progression.
330
331 Prior to the 1960s, the lack of effective treatments and the high incidence of TB created a
332 unique research environment for studying TBI and TBD groups. A 2012 review of 18
333 studies during this time estimated that individuals with TBI had a 79% lower risk of
334 developing active TBD upon reinfection compared to those without prior infection,

335 suggesting the presence of an innate memory-like responses to TB (18). The metabolic
336 shift observed in monocytes from TBI individuals, specifically their enhanced overall
337 metabolic activity and distinct effector function profiles in response to Mtb, may reflect
338 such a memory-like state. These monocytes may have undergone innate immune training,
339 which is a form of innate immune memory characterised by enhanced glycolytic
340 metabolism and effector function (19). Previous studies using BCG or β-glucan to induce
341 trained immunity in monocytes have demonstrated augmented cytokine responses to Mtb,
342 consistent with the findings in our study (20,21).
343
344 The necessity of treating all individuals with TBI is currently debated, with some proposing
345 that people with TBI may have immunological memory despite having already cleared the
346 infection and no longer harbouring viable bacteria (22,23). Our data provide biological
347 evidence supporting the clinical relevance of TBI and the rationale for TPT to actively
348 reverse immunometabolic dysregulation of circulating monocytes. Moreover, our findings
349 also suggest that monocyte MD and metabolic plasticity may represent useful biomarkers
350 of immune status in TB and promising targets for host-directed therapies (HDT) aimed at
351 correcting TB-induced immune dysfunction. Since the metabolic and inflammatory profiles
352 of circulating monocytes influence the function of differentiated macrophages, these cells
353 represent tractable targets for HDT to enhance both peripheral monocyte and lung-
354 resident alveolar macrophage responses to Mtb (24–26). Taken together, our data support
355 the biological relevance of TBI and reinforces the biological rationale for its treatment.
356

357 While our findings offer novel insights into monocyte immunometabolism in TB, this study
358 is not without limitations which include a relatively small sample numbers and the absence
359 of a demonstrated correlation with disease outcomes. Nonetheless, we believe these data
360 provide a compelling foundation for future work. Studies like this are essential for
361 uncovering early immune changes in TB and can inspire larger, mechanistically focused
362 investigations to define new biomarkers and therapeutic targets in host-directed TB
363 research.
364
365 In conclusion, myeloid immunometabolic reprogramming, characterised by reduced MD,
366 occurs early in TB infection and persists without clinical disease. Monocytes from
367 individuals with TBI exhibit memory-like metabolic responses to Mtb, with increased
368 protein synthesis and metabolic plasticity. These features highlight monocytes as potential
369 targets for HDT aimed at restoring metabolic function and supporting memory responses
370 to TB.
371

Acknowledgements

We sincerely thank all the individuals who participated in this study. We are especially grateful to the patients for their time, generosity, and willingness to contribute to research aimed at improving the understanding and treatment of tuberculosis. Their participation made this work possible.

378 ## References

379 1. Geneva WHO. *Global Tuberculosis Report 2024*.; 2024.

380 2. World Health Organisation G. *WHO Consolidated Guidelines on Tuberculosis.*
381 *Module 1: Prevention – Tuberculosis Preventive Treatment, Second Edition*.;
382 2024.

383 3. Coussens AK, Zaidi SMA, Allwood BW, et al. Classification of early tuberculosis
384 states to guide research for improved care and prevention: an international Delphi
385 consensus exercise. *Lancet Respir Med*. 2024;12(6):484-498. doi:10.1016/S2213-
386 2600(24)00028-6/ATTACHMENT/CC7E512D-960D-45EC-8598-
387 A1F924997332/MMC1.PDF

388 4. Sampath P, Moideen K, Ranganathan UD, Bethunaickan R. Monocyte Subsets:
389 Phenotypes and Function in Tuberculosis Infection. *Front Immunol*. 2018;9:1726.
390 doi:10.3389/FIMMU.2018.01726

391 5. Wolf Y, Shemer A, Polonsky M, et al. Autonomous TNF is critical for in vivo
392 monocyte survival in steady state and inflammation. *J Exp Med*. 2017;214(4):905.
393 doi:10.1084/JEM.20160499

394 6. Netea MG, Nold-Petry CA, Nold MF, et al. Differential requirement for the
395 activation of the inflammasome for processing and release of IL-1beta in
396 monocytes and macrophages. *Blood*. 2009;113(10):2324-2335.
397 doi:10.1182/BLOOD-2008-03-146720

398 7. Affandi AJ, Olesek K, Grabowska J, et al. CD169 Defines Activated CD14+
399 Monocytes With Enhanced CD8+ T Cell Activation Capacity. *Front Immunol*.
400 2021;12:697840. doi:10.3389/FIMMU.2021.697840/FULL

401 8. Guilliams M, Mildner A, Yona S. Developmental and Functional Heterogeneity of
402 Monocytes. *Immunity*. 2018;49(4):595-613. doi:10.1016/J.IMMUNI.2018.10.005
403 9. Serbina N V., Pamer EG. Monocyte emigration from bone marrow during bacterial
404 infection requires signals mediated by chemokine receptor CCR2. *Nat Immunol*.
405 2006;7(3):311-317. doi:10.1038/NI1309
406 10. McQuattie-Pimentel AC, Budinger GRS, Ballinger MN. Monocyte-derived Alveolar
407 Macrophages: The Dark Side of Lung Repair? *Am J Respir Cell Mol Biol*.
408 2018;58(1):5-6. doi:10.1165/RCMB.2017-0328ED
409 11. Misharin A V., Morales-Nebreda L, Reyfman PA, et al. Monocyte-derived alveolar
410 macrophages drive lung fibrosis and persist in the lung over the life span. *J Exp*
411 *Med*. 2017;214(8):2387-2404. doi:10.1084/JEM.20162152
412 12. Machiels B, Dourcy M, Xiao X, et al. A gammaherpesvirus provides protection
413 against allergic asthma by inducing the replacement of resident alveolar
414 macrophages with regulatory monocytes. *Nat Immunol*. 2017;18(12):1310-1320.
415 doi:10.1038/NI.3857
416 13. Aegerter H, Kulikauskaite J, Crotta S, et al. Influenza-induced monocyte-derived
417 alveolar macrophages confer prolonged antibacterial protection. *Nat Immunol*
418 *2020 212*. 2020;21(2):145-157. doi:10.1038/s41590-019-0568-x
419 14. Srivastava S, Ernst JD, Desvignes L. Beyond macrophages: the diversity of
420 mononuclear cells in tuberculosis. *Immunol Rev*. 2014;262(1):179.
421 doi:10.1111/IMR.12217
422 15. Cohen SB, Gern BH, Delahaye JL, et al. Alveolar Macrophages Provide an Early
423 Mycobacterium tuberculosis Niche and Initiate Dissemination. *Cell Host Microbe*.

424 2018;24(3):439-446.e4. doi:10.1016/J.CHOM.2018.08.001
425 16. Jameson G, Walsh A, Woods R, et al. Human tissue-resident NK cells in the lung
426 have a higher glycolytic capacity than non-tissue-resident NK cells in the lung and
427 blood. *Proc Natl Acad Sci*. 2024;121(42):2412489121.
428 doi:10.1073/PNAS.2412489121
429 17. Gleeson LE, Sheedy FJ, Palsson-McDermott EM, et al. Cutting Edge:
430 Mycobacterium tuberculosis Induces Aerobic Glycolysis in Human Alveolar
431 Macrophages That Is Required for Control of Intracellular Bacillary Replication . *J*
432 *Immunol*. 2016;196(6):2444-2449. doi:10.4049/jimmunol.1501612
433 18. Andrews JR, Noubary F, Walensky RP, Cerda R, Losina E, Horsburgh CR. Risk of
434 Progression to Active Tuberculosis Following Reinfection With Mycobacterium
435 tuberculosis. *Clin Infect Dis An Off Publ Infect Dis Soc Am*. 2012;54(6):784.
436 doi:10.1093/CID/CIR951
437 19. Netea MG, Domínguez-Andrés J, Barreiro LB, et al. Defining trained immunity and
438 its role in health and disease. *Nat Rev Immunol*. 2020;20(6):375-388.
439 doi:10.1038/s41577-020-0285-6
440 20. Moorlag SJCFM, Khan N, Novakovic B, et al. β-Glucan Induces Protective Trained
441 Immunity against Mycobacterium tuberculosis Infection: A Key Role for IL-1. *Cell*
442 *Rep*. 2020;31(7):107634. doi:10.1016/j.celrep.2020.107634
443 21. Arts RJW, Carvalho A, La Rocca C, et al. Immunometabolic Pathways in BCG-
444 Induced Trained Immunity. *Cell Rep*. 2016;17(10):2562-2571.
445 doi:10.1016/j.celrep.2016.11.011
446 22. Behr MA, Edelstein PH, Ramakrishnan L. Is Mycobacterium tuberculosis infection

447 life long? *BMJ*. 2019;367:l5770. doi:10.1136/bmj.l5770

448 23. Behr MA, Edelstein PH, Ramakrishnan L. Rethinking the burden of latent
449 tuberculosis to reprioritize research. *Nat Microbiol*. 2024;9(5):1157-1158.
450 doi:10.1038/S41564-024-01683-0

451 24. Suzuki H, Hisamatsu T, Chiba S, et al. Glycolytic pathway affects differentiation of
452 human monocytes to regulatory macrophages. *Immunol Lett*. 2016;176:18-27.
453 doi:10.1016/J.IMLET.2016.05.009

454 25. Russell DG, Simwela N V., Mattila JT, Flynn J, Mwandumba HC, Pisu D. How
455 macrophage heterogeneity affects tuberculosis disease and therapy. *Nat Rev*
456 *Immunol*. Published online January 7, 2025. doi:10.1038/S41577-024-01124-3

457 26. Niec RE, Rudensky AY, Fuchs E. Inflammatory adaptation in barrier tissues. *Cell*.
458 2021;184(13):3361-3375. doi:10.1016/J.CELL.2021.05.036

459

460

461 Figure Legends

462 **Figure 1. Monocytes from people with TBI and TBD exhibit enhanced cytokine and**
463 **chemokine output in response to Mtb stimulation compared with HC.** Monocytes
464 were isolated from PBMC and cultured for 18 hrs with and without irradiated H37Rv (Mtb).
465 [Healthy controls (HC, n=5)), latent (TBI, n=8) and Active (TBD, n=5) TB patients]. **A-B)**
466 Mean levels of cytokine and chemokine concentrations (pg/mL) in supernatants collected
467 from unstimulated (A) and Mtb-stimulated (B) monocyte cultures [HC (blue), TBI (light
468 grey) and TBD (dark grey]. **C)** Fold change increase in concentration of analytes when
469 stimulated with Mtb from baseline across all groups. P values calculated using Kruskal
470 Wallis test and Dunn's multiple comparison test.

471

472 **Figure 2. TB infection alters monocyte phenotype with increased CD14 and reduced**
473 **HLADR expression.** PBMC were isolated from peripheral blood and stained for flow
474 cytometry analysis. **A)** Representative flow plot showing gating strategy and bar chart of
475 immune cell frequencies as percentage of total cells. **B)** Representative flow plot of gating
476 strategy and bar chart of monocyte subset frequencies as percentage of total monocytes.
477 **C)** Representative histogram of flow cytometry antibody staining in classical monocytes.
478 **D-F)** MFI values for CD14, HLA-DR, CD45RA, CD40, TNFRI, and TNFRII expression on
479 classical monocytes across HC, TBI and TBD. P values generated using Two-Way ANOVA
480 with Tukey's multiple comparison test and Kruskal Wallis test with Dunn's multiple
481 comparison.

482

483 **Figure 3. Monocyte metabolism is reprogrammed in TB.** PBMC were isolated from
484 peripheral blood and cultured with or without irradiated H37Rv (Mtb) 10ug/mL for 18 hr.
485 Post-18hr PBMC cultures were treated with metabolic inhibitors 2-deoxyglucose (2DG),
486 oligomycin (O), combinations of both (DGO), or a negative control harringtonine (H).
487 Puromycin was then added, and cells were cultured for 40 min. Cells were washed and
488 stained with fluorochrome-conjugated antibodies against CD14 and puromycin and
489 analyzed by flow cytometry. **A)** Representative flow cytometry gating strategy showing
490 the analyses of monocytes and their puromycin staining across metabolic treatments. **B)**
491 Puromycin MFI values in control monocytes (Co) from HC (n=10) and people with TBI
492 (n=10) and TBD (n=8). **C)** Percent mitochondrial dependence (MD), glycolytic capacity
493 (GC), glucose dependence (GD), and fatty acid and amino acid oxidation capacity
494 (FAO/AAOC) of monocytes in across all cohorts. **D)** Puromycin MFI values in control
495 monocytes (Co) dividing people with TBI into those pre-treatment (TBI/-, n=6) and on-
496 treatment (TBI/+, n=4) and people with TBD into those in the intensive phase phase
497 (TBD/I, n=4)) and those in the continuous treatment phase (TBD/C, n=4). **E)** Percent MD
498 in monocytes with cohort division based on treatment status. **F)** Energy map of
499 monocytes across patient cohorts at baseline and in response to Mtb (mean and SD).
500 **G-H)** Change in puromycin MFI values when monocytes are cultured with Mtb in total
501 cohorts (G, HC n=6, TBI n=8, TBD n=6) and with cohort division based on treatment
502 status (H; HC n=6, TBI/- n=5, TBI/+ n=3, TBD/I n=3, TBD/C n=3). **I-K)** Change in MD of
503 monocytes when cultured with Mtb in total cohorts (I) and when people with TBI (J) and
504 TBD (K) are divided based on treatment status. P values generated using Two-Way

505 ANOVA with Tukey's (C), Sidak's (G-I) or Uncorrected Fischer's LSD (J, K) multiple
506 comparison test, Kruskal Wallis test with Dunn's multiple comparison (D, E).

507

508

509 **Supplemental Figure 1. Raw concentration values for monocyte cytokine and**
510 **chemokine production.**
511 Monocytes were isolated from PBMC and cultured for 18 hrs with and without irradiated
512 H37Rv (Mtb). **A-B)** Concentration of cytokines and chemokines (pg/mL) in supernatants
513 collected from unstimulated (A) and Mtb-stimulated (B) monocyte cultures. 2 Way ANOVA
514 with Tukey's multiple comparison test.

515

516 **Supplemental Figure 2. TB infection alters intermediate and non-classical**
517 **monocyte phenotype.**
518 PBMC were isolated from peripheral blood and stained for flow cytometry analysis. **A-B)**
519 MFI values for CD14, HLA-DR, CD45RA, CD40, TNFRI, and TNFRII expression on
520 intermediate (B) and non-classical (B) monocytes across HC, TBI and TBD. P values
521 generated using Two-Way ANOVA with Tukey's multiple comparison test.

522

523

524

525

526

527

528

529 Tables

530

	HC	TBI	TBD
Age	38+-15	44.90+-12.81	41.25+-18.43
Gender	F (9) M (1)	M (11) F (10)	M (10) F (6)
Ethnicity (self-reported)	European (9) African (1)	Asian (10), European (4), African (2), Indian (2), Not reported (3)	Asian (4), European (5), African (7),
Site of Mtb infection	N/A	N/A	Pulmonary (6), Extra-pulmonary (7), Both (2)

531 Table 1: Patient information. HC=Healthy Controls, TBI= Tuberculosis Infection, TBD=

532 tuberculosis disease, F= female, M=male.

533

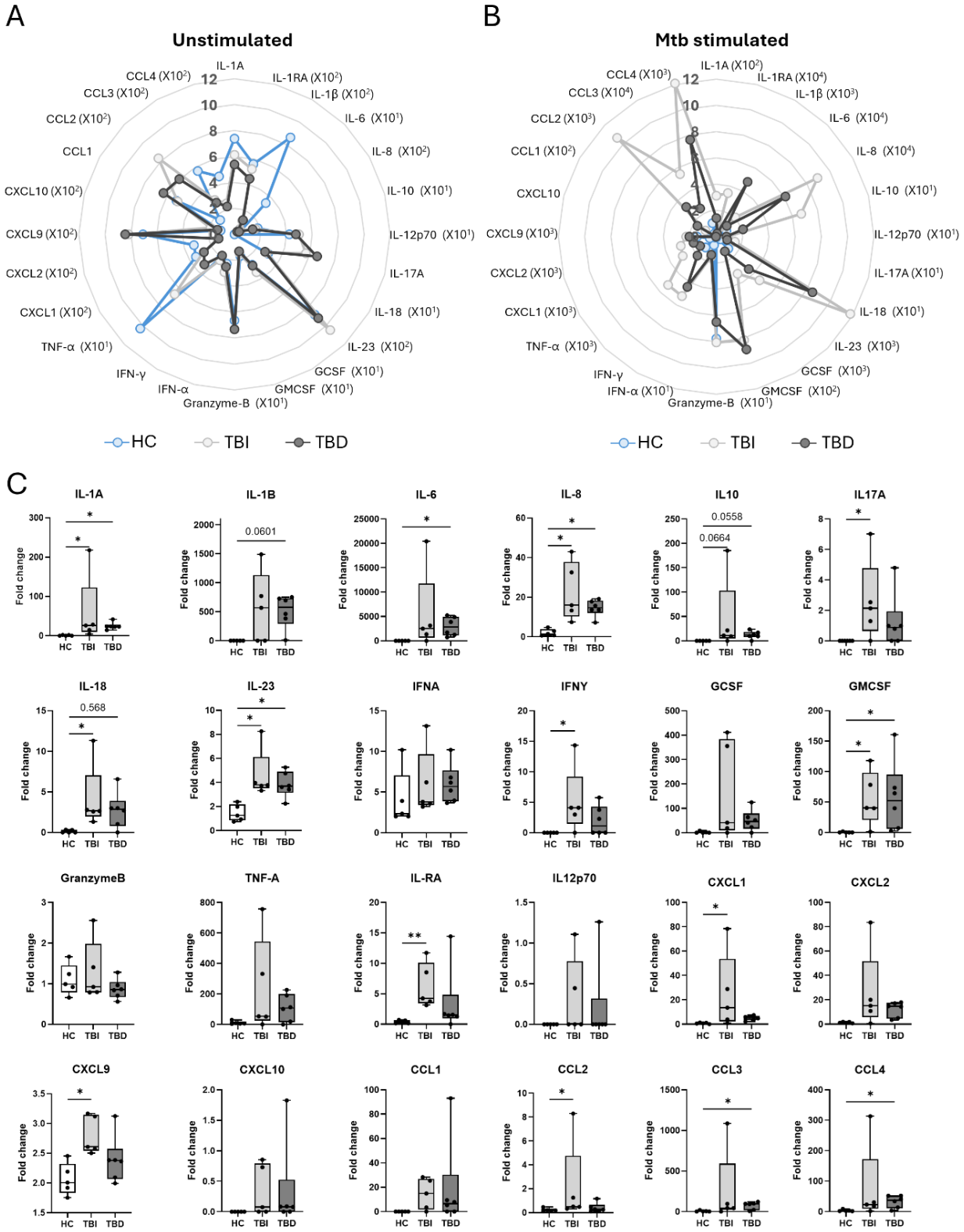
A
Unstimulated
IL-1A
IL-1RA (X10²)
IL-1β (X10²)
IL-6 (X10¹)
IL-8 (X10²)
IL-10 (X10¹)
IL-12p70 (X10¹)
IL-17A
IL-18 (X10¹)
IL-23 (X10²)
GCSF (X10¹)
GMCSF (X10¹)
Granzyme-B (X10¹)
IFN-α
IFN-γ
TNF-α (X10¹)
CXCL1 (X10²)
CXCL2 (X10²)
CXCL9 (X10²)
CXCL10 (X10²)
CCL1
CCL2 (X10²)
CCL3 (X10²)
CCL4 (X10²)
HC
TBI
TBD
B
Mtb stimulated
IL-1A (X10²)
IL-1RA (X10⁴)
IL-1β (X10³)
IL-6 (X10⁴)
IL-8 (X10⁴)
IL-10 (X10¹)
IL-12p70 (X10¹)
IL-17A (X10¹)
IL-18 (X10¹)
IL-23 (X10³)
GCSF (X10³)
GMCSF (X10²)
Granzyme-B (X10¹)
IFN-α (X10¹)
IFN-γ
TNF-α (X10³)
CXCL1 (X10³)
CXCL2 (X10³)
CXCL9 (X10³)
CXCL10
CCL1 (X10²)
CCL2 (X10³)
CCL3 (X10⁴)
CCL4 (X10³)
HC
TBI
TBD
C
IL-1A
IL-1B
IL-6
IL-8
IL10
IL17A
IL-18
IL-23
IFNA
IFNY
GCSF
GMCSF
GranzymeB
TNF-A
IL-RA
IL12p70
CXCL1
CXCL2
CXCL9
CXCL10
CCL1
CCL2
CCL3
CCL4
Fold change
HC
TBI
TBD
0.0601
0.0558
0.0664
0.568

Figure 1

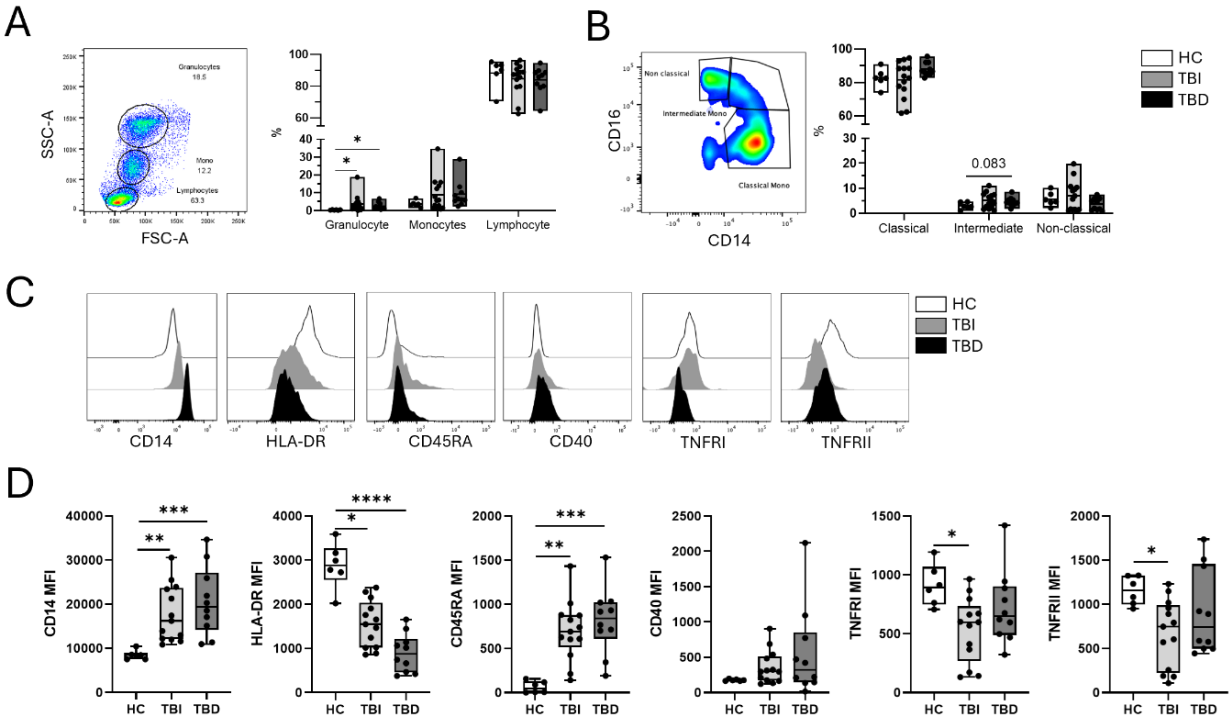

536

537 **Figure 2**

538

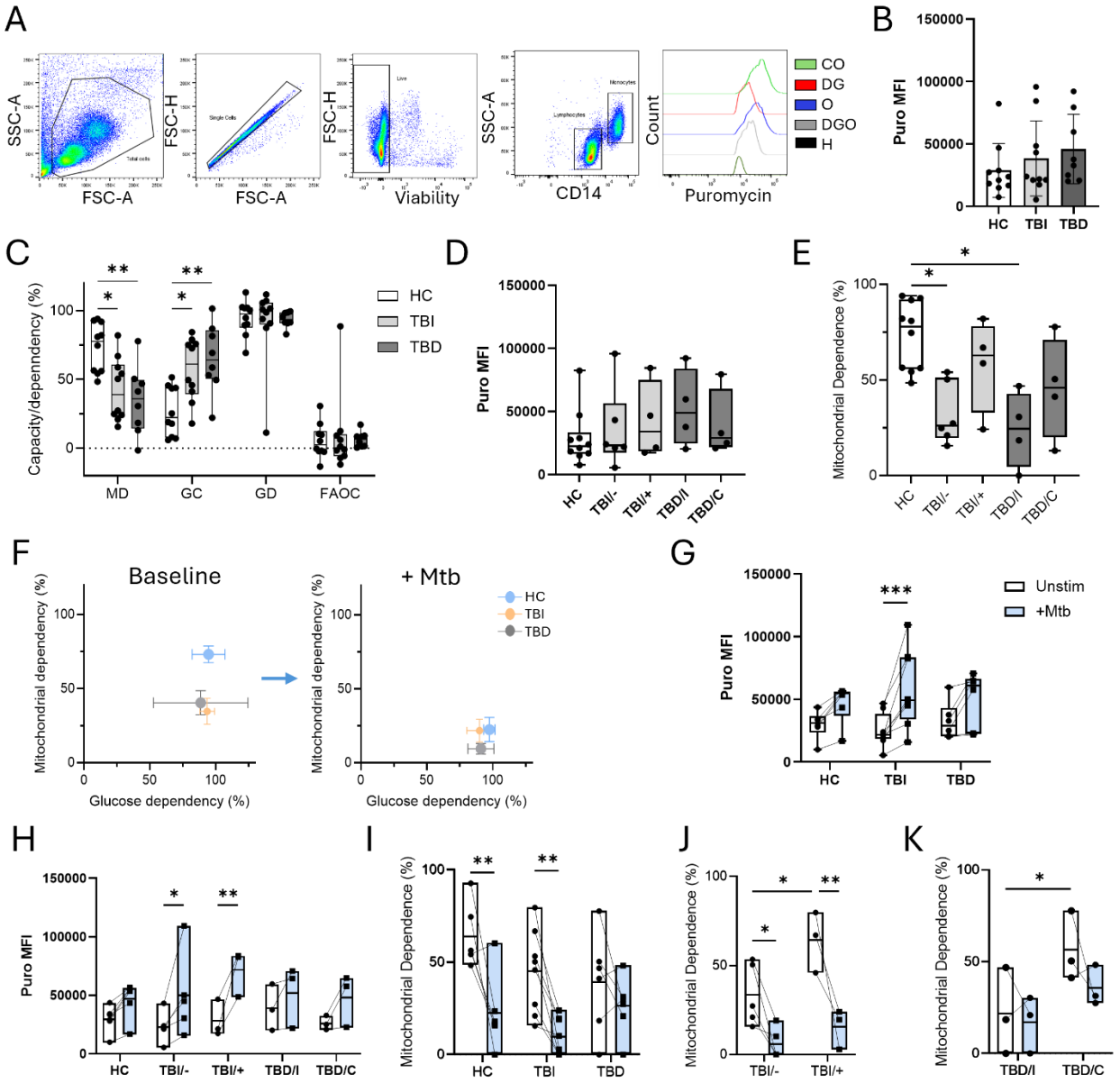
A
SSC-A
FSC-A
FSC-H
FSC-A
FSC-H
Viability
SSC-A
CD14
Count
Puromycin
CO
DG
O
DGO
H
B
Puro MFI
HC
TBI
TBD
C
Capacity/depenndency (%)
MD
GC
GD
FAOC
HC
TBI
TBD
D
Puro MFI
HC
TBI/-
TBI/+
TBD/I
TBD/C
E
Mitochondrial Dependence (%)
HC
TBI/-
TBI/+
TBD/I
TBD/C
F
Baseline
+ Mtb
Mitochondrial dependency (%)
Glucose dependency (%)
HC
TBI
TBD
G
Puro MFI
Unstim
+Mtb
HC
TBI
TBD
H
Puro MFI
HC
TBI/-
TBI/+
TBD/I
TBD/C
I
Mitochondrial Dependence (%)
HC
TBI
TBD
J
Mitochondrial Dependence (%)
TBI/-
TBI/+
K
Mitochondrial Dependence (%)
TBD/I
TBD/C

Figure 3

A

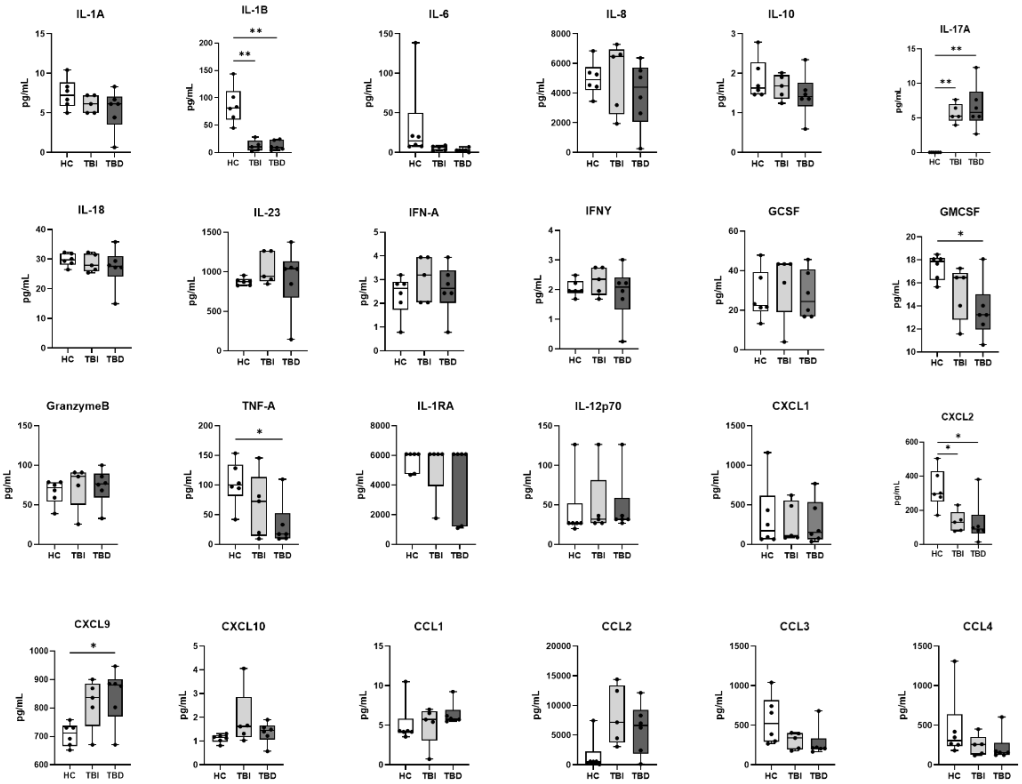
IL-1A
IL-1B
IL-6
IL-8
IL-10
IL-17A
IL-18
IL-23
IFN-A
IFNY
GCSF
GMCSF
GranzymeB
TNF-A
IL-1RA
IL-12p70
CXCL1
CXCL2
CXCL9
CXCL10
CCL1
CCL2
CCL3
CCL4
pg/mL
HC
TBI
TBD

B

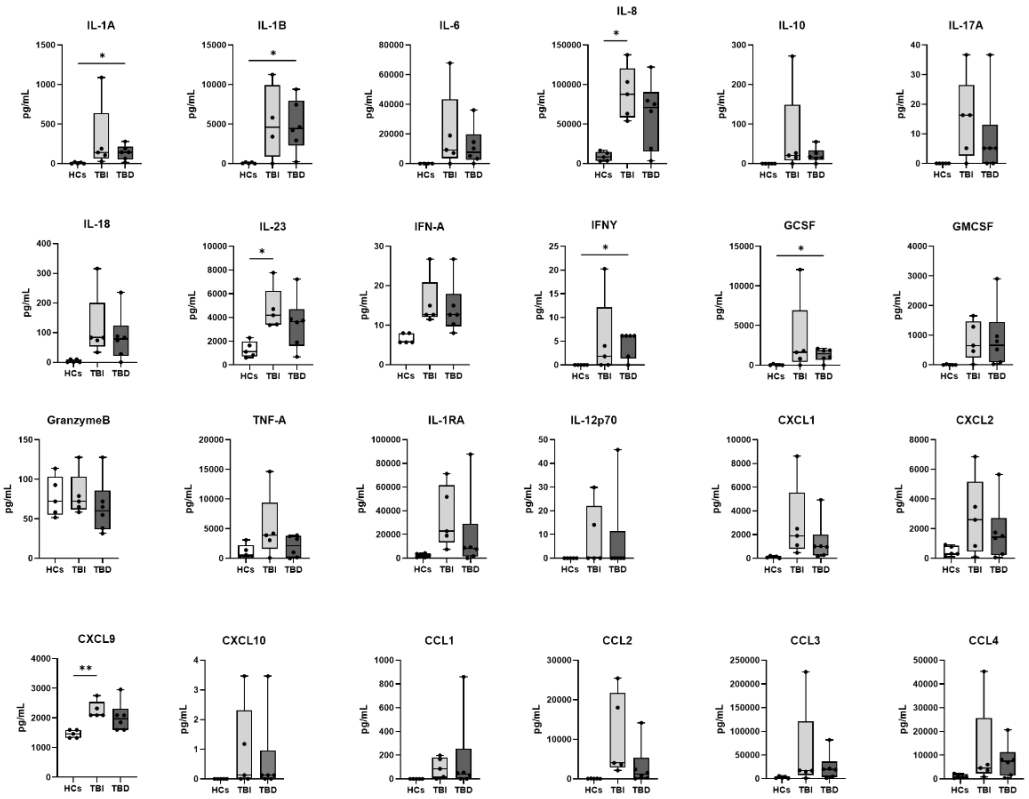
IL-1A
IL-1B
IL-6
IL-8
IL-10
IL-17A
IL-18
IL-23
IFN-A
IFNY
GCSF
GMCSF
GranzymeB
TNF-A
IL-1RA
IL-12p70
CXCL1
CXCL2
CXCL9
CXCL10
CCL1
CCL2
CCL3
CCL4
pg/mL
HCs
TBI
TBD

542

543 **Supplemental Figure 1**

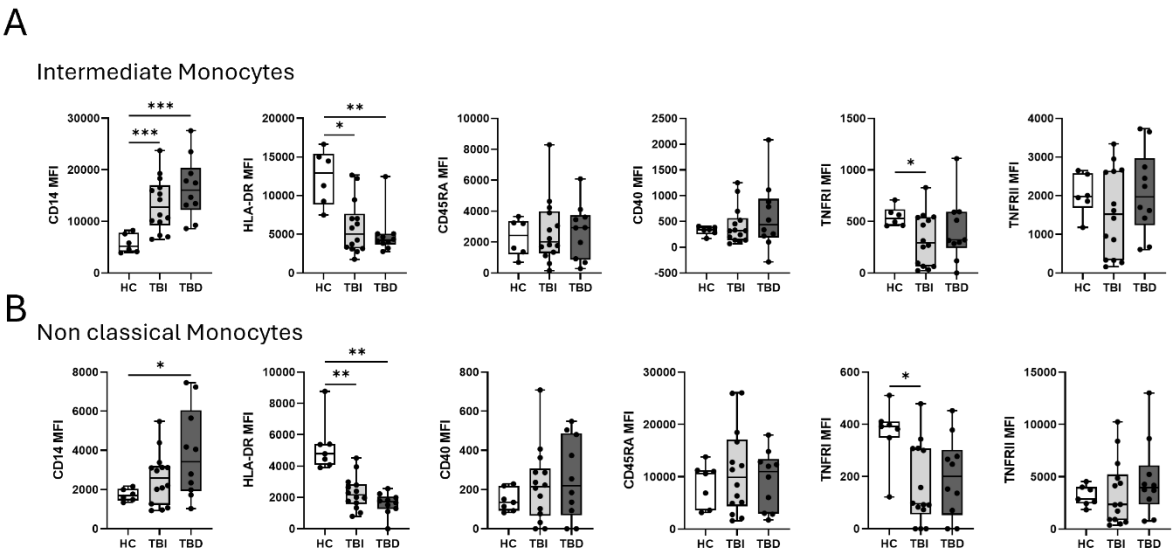

544

545 **Supplemental Figure 2**

546

547